

Evaluation of Intraoperative Radiation Therapy for Unresectable Pancreatic Cancer with FDG PET

Tatsuya Higashi, Harumi Sakahara, Tatsuo Torizuka, Yuji Nakamoto, Shuichi Kanamori, Masahiro Hiraoka, Masayuki Imamura, Yasumasa Nishimura, Nagara Tamaki and Junji Konishi

Departments of Nuclear Medicine and Radiology, First Department of Surgery, Kyoto University Faculty of Medicine, Kyoto; Department of Radiology, Kinki University School of Medicine, Osaka-Sayama, Osaka; and Hokkaido University School of Medicine, Sapporo, Japan

This investigation was undertaken to evaluate ^{18}F -labeled fluorodeoxyglucose (FDG) PET in monitoring patients after intraoperative radiotherapy (IORT) for unresectable pancreatic cancer and to compare its usefulness with CT. **Methods:** FDG PET was performed in 12 consecutive unresectable ductal adenocarcinoma patients before ($n = 12$) and after IORT (0.7–11.9 mo, $n = 14$). In the follow-up period, FDG PET results after IORT were divided into three groups: early (0–2.0 mo after IORT, $n = 7$), intermediate (2.1–4.0 mo, $n = 5$) and delayed period (4.1 mo or later, $n = 2$). FDG uptake at 60 min after injection of 185 MBq FDG under fasting conditions was analyzed with standardized uptake value (SUV). Three parameters, the highest SUV in the tumor, the area of tumor showing SUV of more than 2.0 and the average SUV in the tumor area were calculated. Ratios of each parameter after IORT to that before IORT were defined as residual uptake ratio (RUR)-1, -2 and -3, respectively. Tumor regression after IORT was evaluated with CT as tumor size ratio (TSR) every 2 mo. **Results:** Results of RUR-1 and -3 were consistent with tumor size measured by CT. They decreased in 10 patients with partial response and increased in 2 patients with no change, although these 2 patients had abscesses. RUR-3 decreased consistently as 0.65 ± 0.33 in 2 mo, 0.51 ± 0.39 in 4 mo and 0.24 in 4 mo or later after IORT, respectively. RUR-1 decreased in early period, but demonstrated no change through the remaining periods. There were discrepancies between the results of RUR-2 and those of the other RURs. CT results revealed a slow decrease in tumor size, because TSR was 0.91 ± 0.10 , 0.76 ± 0.11 and 0.70 ± 0.18 in 2, 4 and 6 mo after IORT, respectively. RUR-3 was smaller than TSR at 2 mo ($P < 0.05$) and 4 mo ($P = 0.056$). These results indicate that the measurement of the average SUV in the tumor area with FDG PET could evaluate the local response of pancreatic cancer after IORT earlier and more markedly than with CT. **Conclusion:** FDG PET was useful in monitoring patients after IORT, because the decrease of metabolism in pancreatic tumor could be detected earlier than the decrease in tumor size.

Key Words: pancreatic cancer; intraoperative radiotherapy; treatment effect

J Nucl Med 1999; 40:1424–1433

PET with ^{18}F -labeled fluorodeoxyglucose (FDG) has shown promise in oncologic imaging. An increase in FDG uptake has been demonstrated in various malignant tumors (1–5). FDG PET was also used to monitor the early therapeutic effect in tumors, including head and neck cancer, breast cancer, hepatocellular carcinoma and malignant lymphoma (6–10). For pancreatic tumors, we have reported the clinical values of FDG PET for the detection and differentiation of pancreatic carcinoma (11,12). However, the use of FDG PET in the evaluation of treatment effects in pancreatic cancer has not been fully investigated.

Pancreatic carcinoma is associated with a poor prognosis (13). The poor outcome may result from the fact that in many cases, the tumors are already unresectable at the time of diagnosis (14). Recently, intraoperative radiotherapy (IORT) has been widely used as a high single dose of radiation that can be safely given to tumors. IORT has been confirmed to have a significant effect in relieving pain in patients with localized unresectable pancreatic cancer, although the role in prolonging the survival of patients still remains unclear (14–18). Recent reports showed that tumor regression for pancreatic cancer evaluated with CT after IORT was slow, taking 4 mo to show maximum tumor regression (19). It is worth examining the usefulness of FDG PET as a functional imaging tool in the evaluation of treatment effects of IORT in pancreatic cancer.

In this study, to evaluate the treatment effects of IORT for unresectable human pancreatic cancers, we performed a series of FDG PET studies before and after the IORT operation, examined FDG uptake in comparison with the tumor regression on CT images and also compared the three evaluation methods of FDG PET for treatment effect that were proposed in this study.

MATERIALS AND METHODS

Patients

The study group comprised 12 consecutive patients with suspected unresectable pancreatic tumors (7 men, 5 women; mean age 57 y, age range 42–73 y) who were examined with FDG PET studies between June 1994 and June 1997 at Kyoto University Hospital and who underwent surgical laparotomy with IORT and could undergo both pre- and postoperative FDG PET. Patients who

Received Sep. 10, 1998; revision accepted Mar. 5, 1999.

For correspondence or reprints contact: Tatsuya Higashi, MD, Department of Nuclear Medicine, Kyoto University Faculty of Medicine, Shogoin, Sakyo-ku, Kyoto, 606-01 Japan

had complete or partial resection with IORT were excluded. Patients underwent preoperative FDG PET within 1–2 wk before IORT, and underwent postoperative FDG PET at 0.7–11.9 mo (average 2.53 mo) after the operation at least once. Patients who could not undergo FDG PET after IORT because of poor clinical condition were excluded. The clinical condition of patients 5 and 8 allowed for two FDG PET scans for each patient after IORT. According to the follow-up periods, FDG results after IORT were divided into three groups: early (0–2.0 mo after IORT, n = 7), intermediate (2.1–4.0 mo, n = 5) and delayed (4.1 months or later with an average of 10.0 mo, n = 2). The patients also underwent preoperative CT within 1–2 wk before the operation and were followed postoperatively with a CT study every 2 mo, up to 12 mo after IORT. They all had surgical staging and biopsy at the time of laparotomy, and their histologic diagnoses proved to be adenocarcinoma. Clinical stages according to the 1987 Union Internationale Contre le Cancer staging system were as follows: stage IV, 4 patients; stage III, 7 patients; and stage II, 1 patient. All the patients were treated with IORT (mean dose 25.5 Gy) combined with external beam radiation therapy (EBRT) (mean dose 47.1 Gy) before or after IORT; 8 of 12 patients received additional chemotherapy (Table 1). The methods used to deliver IORT and EBRT were previously described in detail (16).

Diagnosis of abdominal abscess, liver metastasis or peritonitis carcinomatosa was performed by general assessment of clinical conditions, sonography, CT and PET studies, and the laboratory data (such as serum C-reactive protein and CA19–9). Pathologic examination was not performed during the follow-up periods.

Before enrollment in this study, each patient provided written

informed consent, as required by the Kyoto University Human Study Committee.

PET Imaging

Imaging Technique. ^{18}F was produced by ^{20}Ne (d, α) ^{18}F -labeled nuclear reaction, and FDG was synthesized with the acetyl hydrofluorite method (20). PET was performed with an eight-ring, whole-body PET camera (PCT3600W; Hitachi Medico, Tokyo, Japan), which provides 15 tomographic sections at 7-mm intervals. The intrinsic resolution was 4.6-mm full width at half maximum (FWHM) at the center, and the axial resolution was 7-mm FWHM. The effective resolution after reconstruction was approximately 10 mm. The field of view and the pixel size of the reconstructed images were 512 and 4 mm, respectively. Scatter correction was not performed. The patients fasted for at least 5 h before the FDG injection. Plasma levels of glucose were measured at the time of FDG injection.

On the preoperative FDG PET scan, the exact position of pancreatic tumor was verified and marked on the skin as determined by sonography before the time of imaging. The patients were placed in a prone position on the center of the PET camera bed. During the whole imaging procedure, they kept their arms over their head in the same position, aided by a headrest and a holding bar. The exact position of the patient was determined, because the center of the tumor mass was located in the center of the imaging field with a laser beam alignment system. This patient position was marked with a pen in a cross line using the laser beam system. On the preoperative FDG PET scan, the longitudinal distance between the center of the tumor and the caudal edge of the xiphoid process

TABLE 1
Summary of Treatment and Prognosis of 12 Patients with Pancreatic Cancer

Patient no.	Age (y)	Sex	Tumor characteristics		Dose of irradiation (Gy)			Chemotherapy		Prognosis				Outcome
			Stage	Size (mm)	Before IORT	IORT dose	After IORT	Before IORT	After IORT	Re-sponse	Survival (mo)	Local recurrence	Relapsed site	
1	63	M	T3N1M1	60	0	30	40	None	5-FU 5.0 g, CDDP 100 mg	PR	4.05	—	Liver meta	Died
2	47	F	T3N1M0	50	0	12	50.4	None	None	PR	4.10	—	Liver meta	Died
3	45	M	T3N1M1	60	0	30	45	5-FU 3.5 g, Farumorbicin 20 mg	None	PR	4.13	—	P & L	Died
4	72	M	T3N1M0	50	42	25	0	MMC 10 mg, 5-FU 4.0 g	None	NC	6.40	—	Peritonitis	Died
5	51	M	T3N1M0	60	0	28	52.4	MMC 10 mg, 5-FU 4.0 g	None	PR	7.37	—	P & L	Died
6	48	M	T3N1M0	25	0	30	40	None	None	PR	8.77	—	P & L	Died
7	42	M	T3N1M1	100	16.2	14	43.2	None	None	NC	11.13	—	P & L	Died
8	73	F	T3N0M0	60	0	30	50.4	None	None	PR	12.33	—	Liver meta	Died
9	64	F	T3N1M1	80	50.4	14	0	MMC 10 mg, 5-FU 4.0 g	MTX 50 mg, 5-FU 0.5 g	PR	14.03	—	Peritonitis	Died
10	60	F	T3N1M0	50	45	30	0	5-FU 8.5 g, CDDP 127.5 mg	None	PR	17.20	—	Liver meta	Died
11	62	M	T3N1M0	60	0	30	45	5-FU 5.0 g, CDDP 100 mg	None	PR	7.00	—	Liver meta	Alive
12	56	F	T3N1M0	45	45	30	0	5-FU 8.75 g, CDDP 175 mg	None	PR	13.17	—	None	Alive

IORT = intraoperative radiotherapy; FU = fluorouracil; CDDP = cis-diaminedichloroplatinum; PR = partial response; meta = metastasis; P & L = peritonitis and liver metastasis; MMC = mitomycin C; NC = no change; MTX = methotrexate sodium.

or the cephalic edge of the pubic bone of the patient was measured before transmission scanning, which was used for the exact correspondence of the patient position between the pre- and postoperative FDG PET scans. The patient was then held in place with a holding belt across the abdomen.

For postoperative FDG PET, the procedures for the patients' position differed slightly from those used in the preoperative imaging. At first, the patient was positioned in the same prone position on the center of the PET camera bed. The center of the tumor mass was then positioned to be located in the center of the imaging field with the laser beam alignment system and the distance from the bones as previously mentioned. After these procedures, the position of pancreatic tumor was verified by sonography. Again the patient was marked with a pen and held with a holding belt across the abdomen.

Patient positions were kept fixed during transmission scanning for attenuation correction in image reconstruction for 20 min. After the transmission scan, approximately 185 MBq (5.0 mCi) FDG were administered intravenously. About 50–55 min later, the patient were repositioned on the PET camera bed. The marking and the laser beam system were used to ensure that the patient was placed in precisely the same position as in the transmission scan. Exactly 60 min after the FDG injection, static scanning was performed for 15 min (12).

Image Analysis. PET images were compared with the corresponding CT images for accurate anatomic identification of the tumor. On CT images, the longitudinal distances between the center of the tumor, the edge of the xiphoid process and the lower edge of the liver of the patient were calculated by slice thickness. These measurements were used for the exact correspondence of the patient position between FDG PET and CT images.

On the preoperative FDG PET scan, the boundary of the tumor mass could be clearly visualized and assessed by visual comparison. The shape of tumor uptake was usually observed as a focal centripetal strong uptake on the preoperative images. On the postoperative FDG PET scans, however, the shape of tumor uptake changed to an irregularly shaped uptake after IORT, sometimes with multiple high uptake spots along the boundary. In addition, the center of tumor boundary by visual interpretation was sometimes observed in a different image slice compared with the markers, such as the xiphoid process and the lower edge of the liver. However, the longitudinal distance of the tumor center position between pre- and postoperative PET by our corresponding system was within ± 1.5 slices of each other.

Therefore, the evaluation of tumor uptake by FDG PET was performed in seven consecutive imaging slices on both pre- and postoperative PET for the purpose of correcting the possible error due to the longitudinal differences between the slices. The seven slices were determined during preoperative PET so that the center of tumor boundary was located in the center of these slices. On the other hand, the seven slices during postoperative FDG PET were defined by our corresponding system because they were located in the same anatomic position as that in the preoperative images, regardless of the shape of uptake or the longitudinal differences. In one postoperative imaging session (patient 12), a focal high FDG uptake with standardized uptake value (SUV) 3.5 was observed outside the seven consecutive slices, with a distance of five slices from the preoperative center. However, we interpreted this focus as an inflammatory change or nonirradiated lymph node in the extrairradiation field at that time, which was later clinically confirmed to be inflammatory change.

On each of the consecutive seven slices, FDG accumulation was analyzed quantitatively by calculating the SUV in the regions of interest (ROIs) placed over the tumor (21) by three highly experienced physicians as follows:

$$\text{SUV} = \frac{\text{PET count} \times \text{calibration factor (mCi/g)}}{\text{injection dose (mCi)/body weight (g)}}$$

In this study, three parameters, the highest SUV in the tumor area (parameter 1), the area of tumor showing SUV of more than 2.0 (parameter 2) and the average SUV in the tumor area (parameter 3) were calculated. Ratios of each parameter after IORT to that before IORT were defined as residual uptake ratio (RUR)-1, -2 and -3, respectively. This definition derives from the fact that maximum SUV of 2.0–2.2 is considered the threshold between malignant and benign pancreatic tumors in our university (11,21).

Parameter 1 was calculated using an average count in an ROI of 10×10 mm square (independent of tumor size), which was selected in areas of tumor that showed the highest FDG activity in all the consecutive slices. This was the same method used in our previous study and is basically similar to the most common methods used in the evaluation of static FDG PET studies (1,2,11). Although the highest ROI in the preoperative study was always located in the center of the seven consecutive slices, the highest ROI in the postoperative study could be located in another slice within the seven consecutive slices, as previously mentioned. RUR-1 showed the change of the highest uptake point within the tumor area, as follows (Fig. 1):

$$\text{RUR-1} = A'/A,$$

where A = SUV of 10×10 mm ROI before IORT, which was selected in areas of tumor that showed the highest FDG activity, and A' = SUV of 10×10 mm ROI placed as the same way after IORT.

Parameter 2 was measured as the area of tumor showing SUV of more than 2.0. In each consecutive slice, we adjusted the window level manually to clearly reveal the boundary enclosing all pixels with uptake greater or equal to $\text{SUV} = 2.0$ within the seven consecutive slices. These boundaries were then determined as ROI of the tumor area in each slice. The largest ROI boundary having the largest pixel area for the tumor mass in the seven consecutive slices was defined as the area of tumor for parameter 2. Although the largest ROI in the preoperative study was always located in the center of the seven consecutive slices, the largest ROI in the postoperative study could be located in another slice within the consecutive slices. We calculated RUR-2 as the change of pixel area of the appropriate tumor mass, as follows (Fig. 1):

$$\text{RUR-2} = Z'/Y,$$

where Y = the largest number of pixels of the suspected tumor area showing $\text{SUV} = 2.0$ or more before IORT (Y larger than X or Z), and Z' = the largest number of pixels of the suspected tumor area showing $\text{SUV} = 2.0$ or more after IORT (Z' was larger than X' or Y').

We also calculated parameter 3 using the same area of tumor showing SUV of more than 2.0 as used in parameter 2. At first, the largest ROI boundary for the tumor area was defined as the preoperative tumor boundary on preoperative PET, using the same procedure as parameter 2. Then the average uptake count in this ROI boundary was measured. This preoperative ROI boundary was also placed on all the seven consecutive slices on postoperative

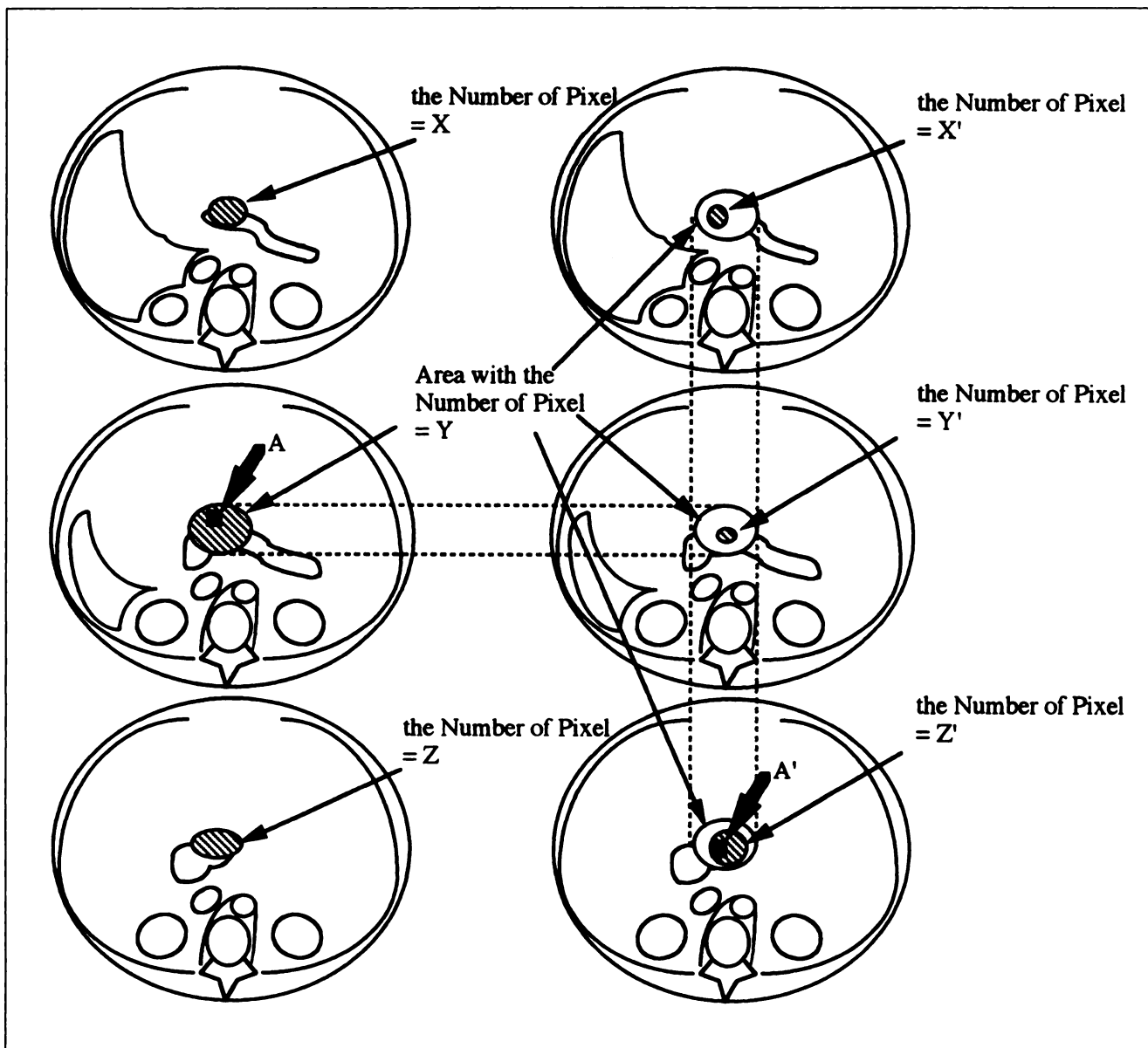


FIGURE 1. Schematic figures of three parameters for comparative FDG PET evaluation of treatment effect. Left three figures represent three consecutive slices of preoperative FDG PET (only three of seven slices we evaluated in this study are presented here). Spot with highest SUV in tumor for parameter 1 (thick arrow, A) and largest area of tumor with SUV > 2.0 for parameters 2 and 3 (shaded circle with number of pixel = Y; in this schema, Y is larger than X or Z) are shown. Both were located in central slice of seven slices. Right three slices represent postoperative PET images and show different uptake pattern. Spot for parameter 1 (thick arrow, A') and largest area for parameter 2 (area with number of pixel = Z'; in this schema, Z' is larger than X' or Y') are observed in another slice. For parameter 3, we applied ROI with pixel = Y (unshaded circle) on all seven consecutive postoperative PET images and examined highest average uptake.

PET, regardless of the shape of uptake, the highest count or the longitudinal difference. The highest average uptake of this ROI boundary in all the consecutive slices of postoperative PET was used for parameter 3. We then calculated RUR-3 as the change of average SUV within the suspected tumor area defined by preoperative FDG PET, as follows:

$$\text{RUR-3} = Q'/Q,$$

where Q = the average SUV in the ROI boundary suspected tumor area before IORT, which was defined as Y for the area of tumor

showing SUV of more than 2.0. Q' = the average SUV in the same tumor area of Y placed on the PET image after IORT.

CT

Every patient fasted overnight before the CT study was performed. CT examinations were performed in the same overhead-arm position. Hi-Speed Advantage (GE Medical Systems, Milwaukee, WI) or CT-W2000 or CT-W3000 (Hitachi Medico) scanners were used. Unenhanced, dynamic and delayed-enhanced images were used. Unenhanced, dynamic and delayed-enhanced images were obtained in all patients. In several patients, unenhanced

images were omitted after IORT. For unenhanced CT, a section collimation of 5–8 mm at 8- to 10-mm intervals was used, and incremental, contiguous, 5-mm-thick scans were also obtained through the pancreas. Dynamic contrast-enhanced CT with 150 mL of nonionic contrast material administered as a bolus injection through a mechanical power injector at a rate of 2–5 mL/s was performed. Scanning started about 35 s after the beginning of the injection. Helical scans were obtained at 7-mm collimation with 1:1 pitch.

Evaluation of Tumor Response by CT

Two highly experienced physicians determined tumor size by maximum length of long axis on the axial CT image showing maximum size of a tumor in every 2 mo up to 12 mo after IORT. The ratio of tumor size after IORT was calculated as the tumor size ratio (TSR) as follows:

$$TSR = D'/D,$$

where D = maximum length of long axis on the axial image showing maximum size of tumor in CT before IORT, and D' = maximum length measured by each CT after IORT.

The term definitions for tumor response were classified as follows: complete response (CR) as disappearance of the tumor, partial response (PR) as a decrease in the tumor size of more than 70% and no change (NC) as less than 70% decrease (22).

Statistical Analysis

The data in this article were presented as values \pm SD. Probability values < 0.05 indicated a statistically significant difference. The nonparametric statistical analysis between the residual ratio of SUV and that of CT were performed by analysis of variance followed by Mann-Whitney *U* test.

RESULTS

Blood glucose levels at the time of FDG injection were measured with averages of 91.4 ± 21.9 and 100.4 ± 13.2 for pre- and postoperative FDG PET studies, respectively (range 58–151 mg/dL). Blood glucose concentration above 120 mg/dL was noted in only 1 patient (patient 12, before IORT).

Prognosis

Table 1 summarizes the treatment and prognosis of the 12 patients studied. PR and NC were observed in 10 and 2 patients, respectively. There was no instance of CR. All patients with increased CA19–9 before IORT showed decreases in their serum CA19–9 after IORT (data not shown). There was no patient with local tumor recurrence during the follow-up period. The average survival was 9.1 ± 4.4 mo. Of the 12 patients, 10 died of liver metastasis or peritonitis carcinomatosa. There was no remarkable correlation observed between initial serum CA19–9 level, the decreased ratio of CA19–9 and the long-term survival of the patient.

PET Imaging Before and After Intraoperative Radiotherapy

Table 2 shows the results of 14 studies of FDG PET after IORT compared with that before IORT using parameter 1

and RUR-1. Decrease of SUV was well correlated with decrease of tumor size. SUV decreased in 10 patients with PR, and SUV increased in 2 patients with NC. In these 2 patients, however, intra-abdominal abscess was diagnosed at the time of the follow-up PET study. There was no remarkable correlation observed between FDG uptake before IORT, the decreased ratio after IORT and the long-term survival of the patient.

Table 2 also shows the diagnosis of liver metastasis by follow-up FDG PET after IORT. In the 14 follow-up PET studies, PET diagnosed liver metastases accurately as follows: 5 true-positive cases, 8 true-negative cases and 1 false-negative case. In 4 true-positive cases, FDG PET initially detected these nodules before CT and sonography could have detected these nodules. Figure 2 shows a patient with liver metastases scanned by FDG PET twice after IORT.

Comparison of Three Parameters Used in FDG PET

Table 3 shows the results of each RUR. In the early follow-up period, all three RURs showed similar decreased ratios. The results of RUR-3 showed a constant decrease in its average through all three periods with relatively small SD. RUR-1 decreased in the early follow-up but demonstrated no change through the remaining periods with

TABLE 2
Results of FDG PET Before and After IORT with Parameter 1 and RUR-1

Patient no.	Response	FDG PET results				
		Before IORT SUV	PET after IORT			RUR-1
			SUV	Months from IORT	Detection of liver metastasis	
1	PR	11.80	5.42	2.17	TP	0.46
2	PR	5.62	4.04	1.03	TN	0.72
3	PR	4.15	0.53	1.90	FN	0.13
4	NC	4.25	4.82	0.73	TN	1.13
5	PR	4.34	3.23	0.83	TN	0.74
2nd PET after IORT			3.2	4.00	TP*	0.74
6	PR	3.97	2.20	2.40	TP*	0.55
7	NC	3.56	5.3	3.27	TN	1.49
8	PR	4.55	2.73	2.23	TN	0.60
2nd PET after IORT			2.63	8.07	TP*	0.58
9	PR	2.60	1.32	1.17	TN	0.51
10	PR	4.29	2.60	11.87	TP*	0.61
11	PR	5.04	3.51	1.00	TN	0.70
12	PR	4.48	2.82	1.70	TN	0.63

IORT = intraoperative radiotherapy; RUR = residual uptake ratio; SUV = standardized uptake value; PR = partial response; TP = true-positive; TN = true-negative; FN = false-negative; NC = no change; TP* = true-positive/PET initially detected metastatic nodules.

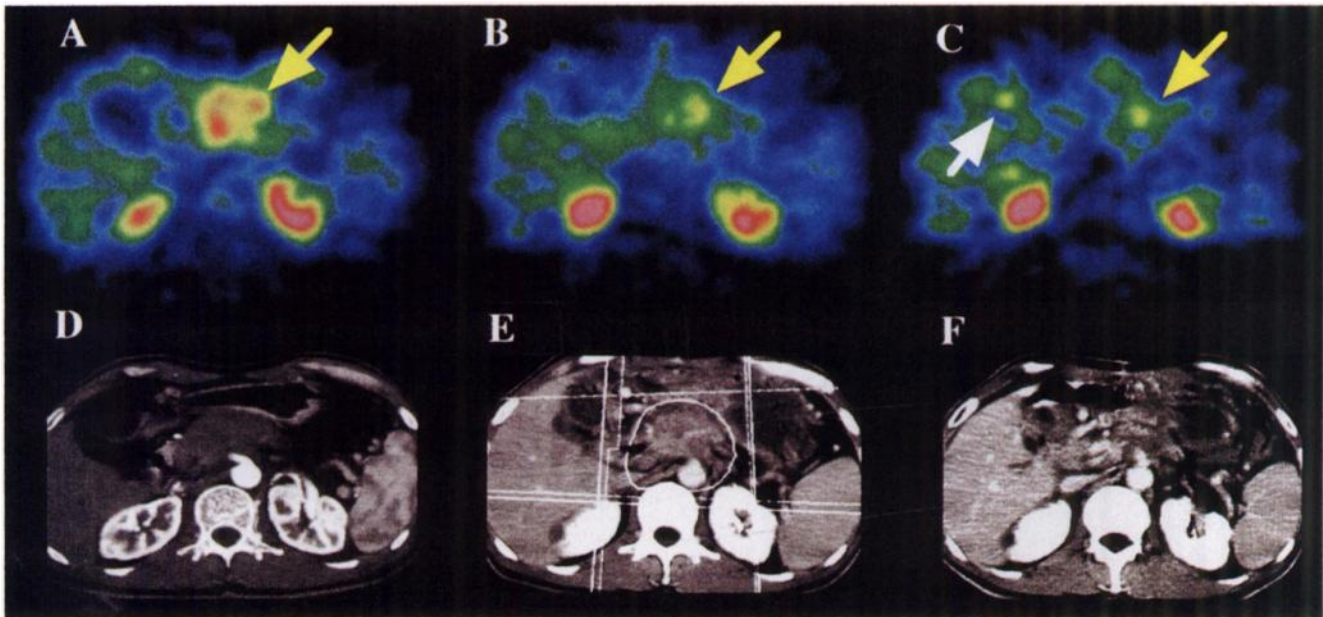


FIGURE 2. Patient 5, 51-y-old man with unresectable ductal adenocarcinoma. (A) PET before IORT shows remarkable focal FDG uptake in pancreatic body (yellow arrow) with maximum SUV = 4.34 using 10 × 10 mm ROI. (B) FDG uptake at 0.83 mo after IORT shows remarkable decreased area of tumor with maximum SUV = 3.23. (C) Follow-up FDG PET at 4.0 mo after IORT shows further decreased high uptake area at tumor site, but maximum SUV was still high (SUV = 3.2). In this intermediate period, liver metastasis was also detected (white arrow). Please note that highest uptake of tumor was observed in one more cephalic side of image in (B) and (C). (D) Contrast-enhanced CT shows low enhanced mass in pancreatic body. (E) Follow-up CT obtained at 0.73 mo after IORT revealed no change. (F) Follow-up CT at 4.0 mo after IORT shows 20% decreased tumor size, whereas it could not detect liver nodule.

relatively small SD. The results of RUR-2 showed fluctuating averages with the largest SD. Furthermore, the RUR-2 results were inconsistent with the other two parameters in 2 patients (patient 1 and 2).

Tumor Size Evaluated by CT

Table 4 shows the tumor response after IORT evaluated as TSR with CT. In the early period, 6 of 12 patients showed no change in tumor size with average TSR of 0.91 ± 0.10 . In

TABLE 3
Comparison Between Each RUR Measured by FDG PET in 12 Patients with Pancreatic Cancer

Early follow-up (n = 7)	Patient no.							Average	SD	
	2	3	4	5	9	11	12			
0–2.0 mo after IORT	1st							Average	SD	
RUR-1	0.72	0.13	1.13	0.74	0.51	0.70	0.63	0.65	0.30	
RUR-2	1.08	0.00	1.68	0.65	0.00	0.65	0.58	0.66	0.59	
RUR-3	0.86	0.15	1.21	0.55	0.50	0.58	0.71	0.65	0.33	
Intermediate follow-up (n = 5)	1	5	6	7	8					
2.1–4.0 mo after IORT	2nd			1st			Average	SD		
RUR-1	0.46	0.74	0.55	1.49	0.60					
RUR-2	1.13	0.58	0.61	1.80	0.33					
RUR-3	0.40	0.21	0.33	1.20	0.43					
Delayed follow-up (n = 2)	8	10								
4.1 mo or more after IORT	2nd							Average		
RUR-1	0.58	0.61							0.60	
RUR-2	0.21	0.49							0.35	
RUR-3	0.25	0.23							0.24	

RUR = residual uptake ratio.

every 2-mo period, TSR revealed a slow and constant decrease with small SD. In the delayed follow-up, TSR nadired in 6 mo or more with TSR of 0.5–0.6.

Comparison Between PET and CT

Figure 3 compares the two parameters of FDG PET (RUR-1 and -3) and TSR measured by CT. No case of discrepancy between decreased FDG uptake measured by PET using RUR-1 and -3 and local tumor response measured by CT appeared. RUR-3 was smaller than TSR in all follow-up periods. RUR-3 was significantly smaller than TSR in 2 mo ($P < 0.05$) and relatively smaller in 4 mo ($P = 0.056$). RUR-1 was significantly smaller than TSR in 2 mo ($P < 0.01$), whereas there was no significant difference between them in 4 mo ($P = 0.27$).

DISCUSSION

These data indicate that the regression of FDG uptake in FDG PET studies was consistent with the local tumor response results evaluated with CT, and that FDG PET detected a decrease in tumor metabolism earlier than tumor size regression. In addition, these data also suggest that in the intermediate and delayed periods after IORT the measurement of average FDG uptake in the suspected tumor area has the potential to evaluate the local tumor response better than that of the maximum FDG uptake in tumor, which is the most common parameter in FDG PET studies. We may say that the local tumor response of pancreatic cancer after IORT could be analyzed by FDG PET within 2 mo, and that it would be better to analyze both the maximum FDG uptake and the averaged FDG uptake in tumor-suspected area, especially in long-term follow-up.

CT Evaluation of Local Tumor Response

The major findings in this study rely on the assumption that good tumor regression measured with CT after IORT

generally means good local control in the evaluation of pancreatic carcinoma treatment. Although tumor size measurement on CT has been the standard method of treatment evaluation in cancer patients, it is difficult to differentiate the residual viable tumor tissue from necrosis or fibrosis clearly on CT. There are only a few articles available to evaluate the early local pathologic response of tumor tissue after IORT (23,24). These reports reveal that the irradiated tumor area consisted of the residual viable tumor tissue, necrosis and fibrosis at first (around 1.5 mo after IORT), and that contraction and scar formation followed this early pathologic change. They suggest that a tumor reduction after IORT cannot be clearly imaged with CT before the process of absorption of necrotic tumor tissue and scar formation. These reports are in agreement with the current results and another report from this group (19). In this study, however, we have no definite pathologic information on this problem. Although there was no patient with local tumor recurrence, 10 of 12 patients died of liver metastasis or peritonitis carcinomatosa. Therefore, even in the good local control cases, we could not deny the possibility that a small number of scattered viable tumor cells could stay buried in the fibrous tissue and that they played an important part for distant metastasis.

Evaluation of Local Tumor Response by FDG PET

The usefulness of FDG uptake for assessing radiotherapy remains a matter of debate (6–10). The decreased FDG uptake of the total irradiated tissue was observed in the early stage after radiotherapy (8,25,26). On the other hand, some articles reveal early phase increased FDG uptake in irradiated tumor cell lines and in irradiated human lymph node metastasis (27,28). It may be said that an accumulation of FDG in irradiated tumor tissue is determined by a result of the “trade-off” of several factors, such as the amount of

TABLE 4
CT Results of Tumor Size Ratio After IORT Compared with Size Before IORT in 12 Patients with Pancreatic Cancer

	Patient no.												Average	SD
	1	2	3	4	5	6	7	8	9	10	11	12		
Early follow-up (n = 12) 0–2.0 mo after IORT	0.80	1.00	1.00	1.00	0.83	0.80	1.00	0.83	1.00	0.80	0.80	1.00	0.91	0.10
Intermediate follow-up (n = 12) 2.1–4.0 mo after IORT	0.67	0.67	0.67	0.80	0.80	0.60	1.00	0.75	0.86	0.80	0.75	0.75	0.76	0.11
Delayed follow-up 1 (n = 9) 4.1–6.0 mo after IORT	ND	ND	ND	0.80	0.67	0.50	1.00	0.50	0.86	0.80	0.67	0.50	0.70	0.18
Delayed follow-up 2 (n = 8) 6.1–8.0 mo after IORT	ND	ND	ND	ND	0.67	0.50	1.00	0.50	0.70	0.70	0.67	0.33	0.63	0.20
Delayed follow-up 3 (n = 6) 8.1–10.0 mo after IORT	ND	ND	ND	ND	ND	0.50	0.80	0.50	0.70	0.50	ND	0.33	0.56	0.17
Delayed follow-up 4 (n = 5) 10.1–12.0 mo after IORT	ND	ND	ND	ND	ND	ND	0.80	0.50	0.67	0.50	ND	0.33	0.56	0.18
Delayed follow-up 5 (n = 1) 12.0 mo after IORT	ND	ND	ND	ND	ND	ND	ND	ND	ND	0.50	ND	ND	0.50	ND

IORT = intraoperative radiotherapy; ND = not done.

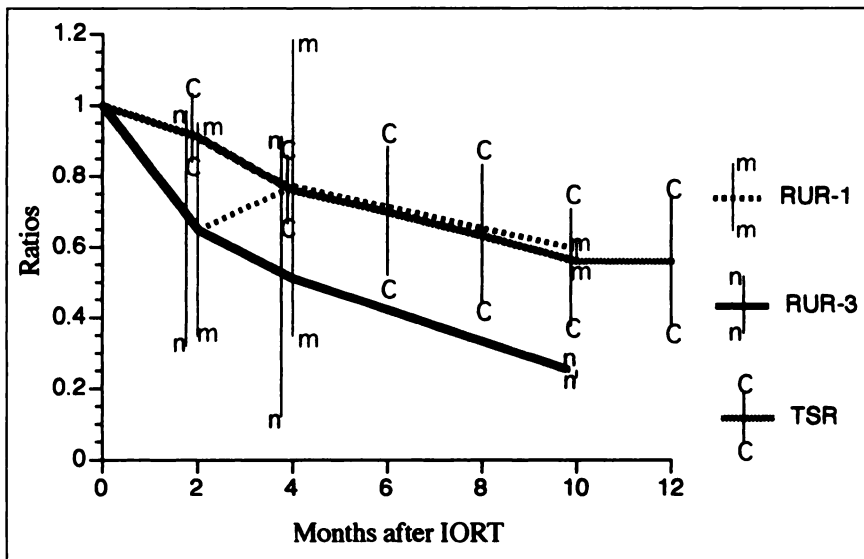


FIGURE 3. Timetable of each parameter measured by FDG uptake (RUR-1 and -3) compared with TSR by CT. Early changes observed in RURs were quick and steep. RUR-3 was decreasing constantly and was smaller than TSR in all follow-up periods, with significant difference in 2-mo periods ($P < 0.05$). RUR-1 decreased quickly and then remained unchanged through all periods. TSR revealed slow and constant decrease with small SD.

uptake by surviving tumor cells, the number of viable tumor cells, the number of inflammatory cells and the change of blood flow or vascular permeability (6,26,29-31). These results are also supposed to depend on several factors, such as dose or method of radiation, time of evaluation, tumor histology, serum glucose level and evaluation method of FDG uptake (6,32). In view of the specific character of this study, three factors should be considered: surviving viable tumor cells, the inflammatory cells and the evaluation method of FDG uptake.

We will begin by considering the problem of surviving viable tumor cells and the evaluation of therapeutic response by FDG PET. The most important point to note is the heterogeneous character of irradiated tumor tissue. As previously mentioned, the shape of tumor uptake became irregularly shaped after IORT, sometimes with multiple high uptake spots in the boundary of the tumor. It does not make sense to think that only a small sample evaluated by one method can be considered representative of the entire, heterogeneous neoplastic tissue. Therefore, it should be said with some emphasis that it is useful in the evaluation of IORT to use multiple methods and to evaluate the character of the method itself.

RUR-1 is important for early detection of local relapse, because it is most commonly used in clinical FDG PET. We should note that both cases of delayed follow-up with relatively higher maximum SUV had liver metastases, and that the only patient with remarkably decreased maximum SUV after IORT (patient 9) was a rare case without liver metastases. One explanation for the remaining higher maximum SUV in delayed follow-up may be the presence of scattered viable tumor cells, as previously mentioned.

Concerning the other two methods we proposed in this study, we were confronted by two difficulties. The first was the accuracy of the corresponding system between pre- and postoperative FDG PET. The second was the validity of

using a single slice for evaluation. We believe our method in this study is justified by the fact that the longitudinal distance of the tumor center position between pre- and postoperative PET imaging was within ± 1.5 slices, and that we evaluated the largest value in the seven consecutive slices.

Comparative results of the three methods showed that there was no remarkable difference among them in the early follow-up period. Therefore, when early response is to be evaluated, it is not problematic to use maximum SUV, which is the most commonly used parameter in clinical FDG PET study. However, the results in the intermediate and delayed periods showed that RUR-3 fairly represents the patients' condition with good local control. We may say that it is better to evaluate the treatment effect not only by the common quantitative analysis using maximum SUV but also by average SUV in tumor-suspected areas, especially in long-term follow-up.

In this study, the definition of ROI boundary for the tumor area was performed using $SUV = 2.0$ within the tumor for parameters 2 and 3. It could be possible to measure these parameters using another value because the threshold varied in each report (1-2). There is room for argument on this point.

The second point is the problem of inflammatory cells. Two cases of follow-up FDG PET showed increased uptake with clinical, not pathologic, diagnosis of abdominal abscess, and PET cannot clearly differentiate between local recurrence of pancreatic cancer and inflammatory change. Several clinical studies report that increased FDG uptake was not lost in most tumors after the treatment, and the residual active tumor could not be distinguished from the inflammatory reaction caused by the radiation (6). Furthermore, it is well known that inflammatory effects occur and may last for the first half year after the end of radiotherapy (33). Although there are only few articles reporting abscess

formation, we should not overlook this inflammatory change (18).

Prognosis

The usefulness of FDG uptake as a predictor of prognosis remains a matter of debate (6–10). The results of this study show that it was impossible to predict the prognosis of unresectable pancreatic cancer with FDG PET. There was no correlation between the initial FDG uptake, the decreased ratio of FDG uptake after IORT and the long-term survival. These results stem partially from the fact that the prognosis of pancreatic cancer is poor and partially from the fact that there was no patient who died of local recurrence in this study. Because patients without follow-up FDG PET were excluded from this analysis, some local recurrence cases might have been excluded because of the clinical condition. In addition, Haberkorn et al. (6) concluded that the differences in treatment response reported in various articles might depend on the tumor types as well as treatment protocols. Further study with more patients is needed.

Another advantage of FDG PET is the detection of metastatic liver nodules. In this study, FDG PET detected 4 cases of liver metastases when CT and sonography could not detect these nodules. The upper portion of liver could not be evaluated by FDG PET because our PET machine has a longitudinal field of view of only 10 cm. A consecutive dual-level scan or whole-body scan that can cover whole liver level would be useful in the evaluation of liver metastases.

CONCLUSION

These data suggest that local tumor response of IORT in unresectable pancreatic cancers can be evaluated earlier with FDG PET than with CT. This could be useful in evaluating local tumor response of IORT not only by the highest SUV in the tumor but also by analysis of the averaged uptake in the preoperative tumor area in the long-term follow-up period.

ACKNOWLEDGMENTS

The authors thank Dr. Yasuhiro Magata, Dr. Satoshi Sasayama, and Haruhiro Kitano of the Department of Nuclear Medicine, Kyoto University Faculty of Medicine, for technical assistance with PET imaging; Richard L. Wahl, MD, of the University of Michigan Medical Center, Ann Arbor, MI, for his supportive advice; and Suzanne Carlson, of the University of Michigan Medical Center, for her valuable assistance.

REFERENCES

1. Bares R, Klever P, Hauptmann S, et al. F-18 fluorodeoxyglucose PET in vivo evaluation of pancreatic glucose metabolism for detection of pancreatic cancer. *Radiology*. 1994;192:79–86.

2. Hawkins RA. Pancreatic tumors: imaging with PET [editorial]. *Radiology*. 1995;195:320–322.
3. Ishizu K, Sadato N, Yonekura Y, et al. Enhanced detection of brain tumors by [¹⁸F]fluorodeoxyglucose PET with glucose loading. *J Comput Assist Tomogr*. 1994;18:12–15.
4. Kubota K, Matsuzawa T, Fujiwara T, et al. Differential diagnosis of lung tumor with positron emission tomography: a prospective study. *J Nucl Med*. 1990;31:1927–1932.
5. Wahl RL, Cody RL, Hutchins GD, et al. Primary and metastatic breast carcinoma: initial clinical evaluation with PET with the radiolabeled glucose analogue 2-[F-18]-fluoro-2-deoxy-D-glucose. *Radiology*. 1991;179:765–770.
6. Haberkorn U, Strauss LG, Dimitrakopoulou A, et al. PET studies of fluorodeoxyglucose metabolism in patients with recurrent colorectal tumors receiving radiotherapy. *J Nucl Med*. 1991;32:1485–1490.
7. Haberkorn U, Strauss LG, Dimitrakopoulou A, et al. Fluorodeoxyglucose imaging of advanced head and neck cancer after chemotherapy. *J Nucl Med*. 1993;34:12–17.
8. Wahl RL, Zasadny K, Helvie M, et al. Metabolic monitoring of breast cancer chemohormonotherapy using positron emission tomography: initial evaluation. *J Clin Oncol*. 1993;11:2101–2111.
9. Nagata Y, Yamamoto K, Hiraoka M, et al. Monitoring liver tumor therapy with [¹⁸F]FDG positron emission tomography. *J Comput Assist Tomogr*. 1990;14:370–374.
10. Okada J, Yoshikawa K, Imazeki K, et al. The use of FDG PET in the detection and management of malignant lymphoma: correlation of uptake with prognosis. *J Nucl Med*. 1991;32:686–691.
11. Inokuma T, Tamaki N, Torizuka T, et al. Evaluation of pancreatic tumors with positron emission tomography and F-18 fluorodeoxyglucose: comparison with CT and US. *Radiology*. 1995;195:345–352.
12. Inokuma T, Tamaki N, Torizuka T, et al. Value of fluorine-18-fluorodeoxyglucose and thallium-201 in the detection of pancreatic cancer. *J Nucl Med*. 1995;36:229–235.
13. Warshaw A, Fernandez-Del Castillo C. Pancreatic carcinoma. *N Engl J Med*. 1992;326:455–465.
14. Shibamoto Y, Nishimura U, Abe M. Intraoperative radiotherapy and hyperthermia for unresectable pancreatic cancer. *Hepato-gastroenterology*. 1996;43:326–332.
15. Nishimura Y, Hosotani R, Shibamoto Y, et al. External and intraoperative radiotherapy for resectable and unresectable pancreatic cancer: analysis of survival rates and complications. *Int J Radiat Oncol Biol Phys*. 1997;39:39–49.
16. Shibamoto Y, Manabe T, Baba N, et al. High dose, external beam and intraoperative radiotherapy in the treatment of resectable and unresectable pancreatic cancer. *Int J Radiat Oncol Biol Phys*. 1990;19:605–611.
17. Kokubo M, Nishimura Y, Nagata Y, et al. Dose-volume histogram analysis of external-beam irradiation combined with IORT for unresectable pancreatic cancer. *Front Radiat Ther Oncol*. 1997;31:177–180.
18. Zerbi A, Fossati V, Parolini D, et al. Intraoperative radiation therapy adjuvant to resection in the treatment of pancreatic cancer. *Cancer*. 1994;73:2930–2935.
19. Kanamori S, Nishimura Y, Kokubo M, et al. CT changes following IORT for unresectable pancreatic cancer. *Front Radiat Ther Oncol*. 1997;31:189–192.
20. Woodard HQ, Bigler RE, Freed B. Expression of tissue isotope distribution [letter]. *J Nucl Med*. 1975;16:958–959.
21. Higashi T, Tamaki N, Honda T, et al. Expression of glucose transporters in human pancreatic tumors compared with increased FDG accumulation in PET study. *J Nucl Med*. 1997;38:1337–1344.
22. *WHO Handbook for Reporting Results of Cancer Treatment*. Geneva, Switzerland: World Health Organization; 1979.
23. Hoekstra HJ, Restrepo C, Kinsella TJ, et al. Histopathological effects of intraoperative radiotherapy on pancreas and adjacent tissues: a postmortem analysis. *J Surg Oncol*. 1988;37:104–108.
24. Nishimura A, Itoh I, Mouri Y, et al. Computed tomography in the assessment of pancreatic tumor response after intraoperative radiation therapy. *Acta Radiol Oncol*. 1986;25:121–126.
25. Kubota K, Ishiwata K, Kubota R, et al. Tracer feasibility for monitoring tumor radiotherapy: a quadruple tracer study with fluorine-18-fluorodeoxyglucose or fluorine-18-fluorodeoxyuridine, L-[methyl-¹⁴C]methionine, [³H]thymidine, and gallium-67. *J Nucl Med*. 1991;32:2118–2123.
26. Higashi K, Clavo AC, Wahl RL. In vitro assessment of 2-fluoro-2-deoxy-D-glucose, L-methionine and thymidine as agents to monitor the early response of a human adenocarcinoma cell line to radiotherapy. *J Nucl Med*. 1993;34:773–779.
27. Furuta M, Hasegawa M, Hayakawa K, et al. Rapid rise in FDG uptake in an irradiated human tumour xenograft. *Eur J Nucl Med*. 1997;24:435–438.

28. Hautzel H, Muller-Gartner HW. Early changes in fluorine-18-FDG uptake during radiotherapy. *J Nucl Med.* 1997;38:1384–1386.
29. Kubota R, Kubota K, Yamada S, et al. Microautoradiographic study for the differentiation of intratumoral macrophages, granulation tissues and cancer cells by the dynamics of fluorine-18-fluorodeoxyglucose uptake. *J Nucl Med.* 1994;35:104–112.
30. Kalfass E, Kramling HJ, Schultz-Hector S. Early inflammatory reaction of the rabbit coeliac artery wall after combined intraoperative (IORT) and external (ERT) irradiation. *Radiother Oncol.* 1996;39:167–178.
31. Senekowitsch-Schmidtke R, Matzen K, Truckenbrodt R, et al. Tumor cell spheroids as a model for evaluation of metabolic changes after irradiation. *J Nucl Med.* 1998;39:1762–1768.
32. Torizuka T, Zasadny KR, Recker B, et al. Untreated primary lung and breast cancers: correlation between F-18 FDG kinetic rate constants and findings of in vitro studies. *Radiology.* 1998;207:767–774.
33. Perez CA, Brady LW, eds. *Principles and Practice of Radiation Oncology.* Philadelphia, PA: JB Lippincott; 1987.